Nanotechnology **22** (2011) 265701 (6pp) doi:10.1088/0957-4484/22/26/265701

Influence of the length and grafting density of PNIPAM chains on the colloidal and optical properties of quantum dot/PNIPAM assemblies

Oya Tagit[1,2], Nikodem Tomczak[3], Aliakbar Jafarpour[1], Dominik Jańczewski[3], Ming Yong Han[3,4], G Julius Vancso[2] and Jennifer L Herek[1]

[1] Optical Sciences, Faculty of Science and Technology and MESA$^+$ Institute for Nanotechnology, University of Twente, PO Box 217, 7500 AE Enschede, The Netherlands
[2] Materials Science and Technology of Polymers, Faculty of Science and Technology and MESA$^+$ Institute for Nanotechnology, University of Twente, PO Box 217, 7500 AE Enschede, The Netherlands
[3] Institute of Materials Research and Engineering, A*STAR (Agency for Science, Technology and Research), 3 Research Link, 117602, Singapore
[4] Division of Bioengineering, Faculty of Engineering, National University of Singapore, 117576, Singapore

E-mail: J.L.Herek@utwente.nl

Received 13 December 2010, in final form 6 April 2011
Published 17 May 2011
Online at stacks.iop.org/Nano/22/265701

Abstract
Structural and optical characterization of water soluble, thermo-responsive quantum dot/poly(*N*-isopropyl acrylamide) (QD/PNIPAM) hybrid particles using fluorescence correlation spectroscopy (FCS) and time-correlated single photon counting (TCSPC) measurements performed at temperatures below and above the lower critical solution temperature (LCST) of PNIPAM is reported. By increasing the temperature above the LCST, the signature of the PNIPAM chain collapse covering the QDs is revealed by FCS measurements. Despite the significant structural change, the TCSPC measurements show that the fluorescence lifetimes remain of the same order of magnitude at $T >$ LCST. Such QD/PNIPAM hybrid particles with water solubility and robust thermo-responsive behavior at physiologically relevant temperatures are potentially useful for (bio)molecular sensing and separation applications.

S Online supplementary data available from stacks.iop.org/Nano/22/265701/mmedia

1. Introduction

The unique optical properties of quantum dots (QDs), such as a broad absorption spectrum and a narrow, size-tunable emission wavelength [1, 2], make them attractive for many applications in life sciences and optoelectronics [3, 4]. Recently, integration of stimulus-responsive polymers with QDs has been pursued in an attempt to create smart, nanosized hybrid luminescent materials [5–10]. In such materials, the physical or chemical properties of the polymer change in response to environmental conditions, such as temperature, pH, ionic strength, or electromagnetic radiation [11], which in turn modulate the photophysical properties of the QDs. Poly(*N*-isopropyl acrylamide) (PNIPAM) is a well-known example of a thermo-responsive polymer exhibiting a lower critical solution temperature (LCST). Below the critical temperature PNIPAM is hydrophilic and disperses well in aqueous solutions. Above the LCST (around 32 °C), it becomes hydrophobic, which is accompanied by deswelling and chain collapse [12]. Fortuitously, the phase transition of PNIPAM occurs in the physiological temperature range, making the polymer especially promising for biological applications [13], such as

drug delivery systems [14], substrates for cell cultures [15] and scaffolds for tissue engineering [16].

The optical characterization of QDs and QD/polymer assemblies as a function of temperature has been studied mostly by absorption and emission measurements [17], while the colloidal properties, such as particle size, distribution and aggregation behavior, have been monitored mostly by light scattering and transmission electron microscopy (TEM) measurements [18]. Conventional light scattering measurements of QDs lack single molecule sensitivity, and bulk measurements can be influenced by aggregation of the nanoparticles [19]. TEM measurements give accurate and quantitative size values; however, it is not possible to study the materials in solution and at high temperatures with this technique. Therefore, it is necessary to use complementary techniques to determine the colloidal and optical properties of temperature-responsive QD/polymer hybrid assemblies [20] at different temperatures.

Fluorescence correlation spectroscopy (FCS) is a sensitive optical detection method with a wide range of applications [21–25]. FCS is based on the measurement of the fluorescence fluctuations as a light emitter passes through the confocal volume. FCS has been employed to determine the diffusion behavior of fluorescent nanoparticles [18, 26, 27], including Si nanoparticles and QDs [19, 28, 29], and to study the formation of polymer micelles [30]. FCS is a particularly attractive method for studying the optical and colloidal properties of engineered QDs for situations where changes in the surface coating may affect both the colloidal and photophysical properties of the QDs, e.g., for QDs coated with thermo-responsive polymers as a function of temperature.

The complementary technique time-correlated single photon counting (TCSPC) allows measurements of fluorescence decay profiles [31]. TCSPC has been widely used for the characterization of colloidal semiconductor nanoparticles [32], organic fluorophores [33], and molecules labeled with fluorescent moieties [34] with picosecond time resolution down to the single molecule level [35].

In this paper, we report on the optical characterization of QD/PNIPAM hybrid assemblies prepared using an amphiphilic coating, at temperatures below and above the LCST of PNIPAM, using FCS and TCSPC. These techniques give novel insights into the colloidal and optical properties of the investigated systems as a function of temperature.

2. Materials and methods

The synthesis of CdSe/ZnS core/shell QDs and grafting of poly(isobutylene-*alt*-maleic anhydride) ($M_w = 6000$ g mol^{-1}, $M_w/M_n = 1.7$, Sigma-Aldrich) with n-octylamine (Sigma-Aldrich) and amino-terminated PNIPAM (NH_2-PNIPAM, Polymer Source Inc., Canada) was performed as described in [20]. Briefly, NH_2-PNIPAM with three different molar masses (M_n), 1000 g mol^{-1}, $M_w/M_n = 1.8$ (P1); 10 800 g mol^{-1}, $M_w/M_n = 1.55$ (P10); and 25 400 g mol^{-1}, $M_w/M_n = 2.49$ (P25), was added into three separate reaction vessels containing tetrahydrofuran (THF) solution of n-octylamine, *N*,*N*-diisopropylethylamine (DIPEA) and poly(isobutylene-*alt*-maleic anhydride) and stirred until a clear solution was obtained. The reaction was left to proceed for 12 h at 50 °C. Further details of the synthesis and purification of the polymers can be found in [20]. ^{1}H NMR studies (see supporting information available at stacks.iop.org/Nano/22/265701/mmedia) revealed that around 19%, 3%, and 0.4% of the poly(isobutylene-*alt*-maleic anhydride) chains had the P1, P10 and P25 polymers attached, respectively. The polymer and QD solutions were mixed while purging with argon. Following the evaporation of THF and half of the volume of water, the solutions were diluted with 2 ml of water. The resulting aqueous solutions of polymer-coated QDs R1, R10 and R25 were filtered through a 0.22 μm MILEX PES membrane filter and centrifuged at 10 000 rpm for 30 min.

FCS measurements were performed using a Confo-Cor2/LSM510 microscope (Carl Zeiss, Germany). Excitation light was provided by a He–Ne laser (543 nm). The laser power was set at approximately 2 μW. Light was focused onto the sample and the luminescence was collected using a water immersion C-Apochromat 40× objective lens with a numerical aperture of 1.2 (Carl Zeiss, Germany), and detected using two fiber coupled avalanche photodiodes. AIM software (Zeiss–EMBL) was used for the autocorrelation analysis. The theory of FCS has been described elsewhere [23, 25, 36]. Briefly, the fluorescence fluctuations around the average intensity, $\delta I(t)$, are monitored and correlated to the intensity obtained at time $t+\tau$ to generate an autocorrelation function. Normalization of the autocorrelation function yields equation (1):

$$G(\tau) = 1 + \frac{\langle \delta I(t)\delta I(t+\tau)\rangle}{\langle I(t)\rangle^2}. \tag{1}$$

The normalized autocorrelation function of the fluorescence fluctuations resulting from the diffusion of the particles through the confocal volume, $G(\tau)$, is used to obtain information about the number of particles per detection volume and the characteristic timescale of diffusion. Assuming a Gaussian profile for the optical excitation source $G(\tau)$ will have the closed-form solution as shown in equation (2):

$$G(\tau) = 1 + \frac{1}{N}\left(1 + \frac{\tau}{\tau_D}\right)^{-1}\left(1 + S^2\frac{\tau}{\tau_D}\right)^{-\frac{1}{2}} \tag{2}$$

where N represents the number of fluorophores in the confocal volume at any time, τ_D is the diffusion time of the molecule through the confocal volume, and S is the structure parameter. S is equal to the ratio of axial (ω_z) and radial (ω_r) distances at which the intensity of the Gaussian excitation falls to e^{-2} of its maximum [18], or simply the aspect ratio of the excitation beam. The inverse relation between the autocorrelation signal and the number of fluorophores enables measurements in the nanomolar range. Data analysis was performed on a PC workstation equipped with an FCS Data Processor 1.4 (Scientific Software Technologies Software Center, Belarus), which allows global fitting using an autocorrelation function describing three-dimensional diffusion with triplet state kinetics. The volume of the confocal spot was determined using a solution of 50 nM Rhodamine 110 with known diffusion coefficient ($D = 420$ μm^2 s^{-1}).

Figure 1. Schematic representation of QD/polymer hybrid structures. Left: R1 (lowest molecular weight PNIPAM with highest grafting density); middle: R10 (moderate molecular weight PNIPAM with moderate grafting density); right: R25 (highest molecular weight PNIPAM with lowest grafting density).

(This figure is in colour only in the electronic version)

Time-resolved fluorescence data were obtained at an emission wavelength of 640 nm by using a HORIBA Jobin Yvon FluoroMax-4 equipped with a NanoLED pulsed laser diode excitation source from IBH (FWHM ∼1 ns, 462 nm) and a TCSPC detection system (FluoroHub, HORIBA Jobin Yvon) based on time to amplitude conversion (TAC). The fluorescence time-resolved data were fitted by using the DAS6 Decay Analysis Software package from HORIBA Jobin Yvon. An instrument response function was recorded on strongly scattering particles (Ludox) in water by using identical settings to those used when measuring the samples; only the emission wavelength was adjusted. Deconvolution analysis of the luminescence decay with three exponentials was carried out. The data were recorded at 20 and at 55 °C. The details of the temperature-dependent steady-state absorption and emission measurements were described in [20]. Dynamic light scattering (DLS) measurements were performed using a Zetasizer Nano ZS (Malvern Instruments, Malvern, UK) equipped with a He–Ne laser (633 nm, 4 mW).

3. Results and discussion

The QDs exhibited a broad absorption spectrum with a first absorption peak at ∼620 nm and a narrow emission spectrum (35 nm full width at half maximum) located at 638 nm. Coating the QDs with the polymer did not induce any noticeable changes in the positions of the absorption and emission peaks; however, the fluorescence intensity was observed to decrease compared to that of the bare QDs in chloroform at the same concentration. Such loss of intensity upon transferring the QDs from organic solvents to water has also been reported previously [37].

The polymers that were used for coating samples R1, R10 and R25 had different contents of PNIPAM chains, of 19%, 3%, and 0.4%, respectively, as determined by ^{1}H NMR. Therefore, in addition to different molar masses of the PNIPAM chains, the grafting densities of PNIPAM chains per poly(isobutylene-*alt*-maleic anhydride) backbone were also different (figure 1). The highest weight percentage of PNIPAM, as inferred from table SI1, belonged to sample R10 (see supporting information available at stacks.iop.org/Nano/22/265701/mmedia).

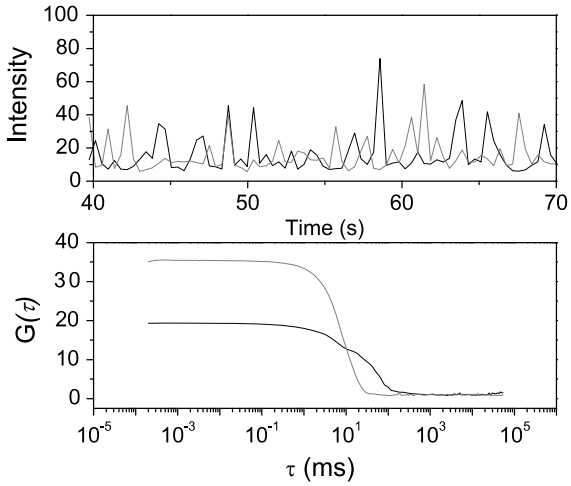

Figure 2. Raw correlation curves and intensity–time-traces of sample R10 measured at T < LCST (black) and T > LCST (gray).

A representative raw data set of FCS, showing the intensity–time-traces and corresponding correlation curves for QDs coated with thermo-responsive PNIPAM at temperatures below (20 °C) and above (55 °C) the LCST is shown in figure 2. Comparison of the raw data for each sample (only R10 is shown here) obtained at T < LCST and T > LCST shows noticeable changes in the shape and amplitude of the correlation curves.

Crossing the LCST resulted in higher amplitudes and steeper slopes of the correlation curves. Considering the inverse relation between the autocorrelation intensity (G_0) and the number of particles within the detection volume (N) (equation (2)), the observed increase in the amplitudes of the correlation curves at T > LCST can be explained by the decrease of the luminescence intensity of the particles or the different excitation laser power. Previously it was shown that the amplitudes of the FCS curves for CdTe QD solutions increase upon addition of a quencher [38]. Such increase of the amplitudes was explained by a decrease in the number of bright QDs present in the solution, causing the apparent number of molecules in the confocal volume to decrease, giving rise to higher amplitudes. At higher intensities the autocorrelation intensity (G_0) was reported to drop due to

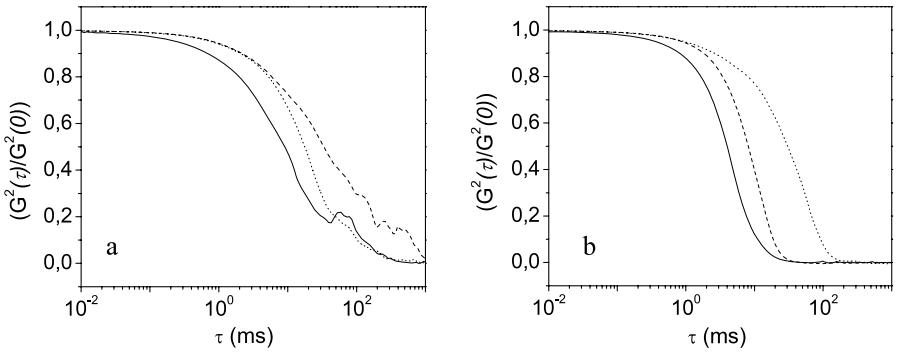

Figure 3. Normalized correlation functions of R1 (——), R10 (– – –) and R25 (· · · · · ·) measured at (a) T < LCST (20 °C) and (b) T > LCST (55 °C).

excitation saturation [39, 40]. However, in our measurements the excitation laser power was kept constant to compare the effects of the different coatings, and to disentangle the intensity dependence of the FCS curve. The potential artifacts that would be introduced due to heating were eliminated by considering the temperature-induced changes in the physical parameters, such as viscosity of water, in our calculations. Therefore, it is likely that the temperature-induced changes to the correlation curves are due to changes in the structure or properties of the QD/PNIPAM hybrids. The steady-state fluorescence emission measurements performed at T > LCST showed that the luminescence intensity of the hybrid particles decreases at T > LCST [20]. Such a decrease in the luminescence intensity at T > LCST is most likely the reason for the higher amplitudes observed in the FCS autocorrelation curves upon crossing the LCST.

The $G(\tau)$ functions used to obtain the diffusion times were averaged over five measurements, and normalized to $G(0) = 1$ for each sample. In parallel, Rhodamine 110 with known molecular weight and diffusion coefficient was used as a calibration standard. The autocorrelation curve obtained for Rhodamine 110 (see supporting information available at stacks.iop.org/Nano/22/265701/mmedia) enabled determination of the radius of the confocal volume.

The correlation curves obtained at T > LCST (figure 3(b)) had steeper slopes when compared to those obtained at T < LCST (figure 3(a)). It has previously been shown that the widths of the correlation functions increase with the increasing molecule size [38], i.e., the characteristic diffusion times of the molecules are positively correlated with their sizes.

The diffusion times of the samples were determined using the slopes of the autocorrelation curves. At T > LCST, the hybrid particles were observed to diffuse faster through the confocal volume, as indicated by the sharper decay in the correlation functions. In addition, the diffusion times of the nanoparticles increased as a function of PNIPAM chain size grafted to the QD coatings.

The diffusion coefficients of the samples at temperatures below and above the LCST of PNIPAM were calculated using equation (3):

$$\tau_D = \frac{\omega_0^2}{4D} \quad (3)$$

Table 1. Diffusion coefficients of R1, R10 and R25 at T < LCST and T > LCST as calculated from FCS correlation curves.

	Diffusion coefficient $D(\times 10^{-12}$ m^2 s$^{-1})$		
	R1	R10	R25
T < LCST	1.4	0.3	0.98
T > LCST	7.7	4.9	1.00

where τ_D is the diffusion time of the particles through the confocal volume, ω_0 is the radius of the confocal volume, and D is the diffusion coefficient. The calibration standard Rhodamine 110 has a known diffusion coefficient, which enabled calculation of ω_0 by inserting the τ_D obtained for Rhodamine 110 into equation (3).

The diffusion coefficients obtained for each sample at temperatures below (20 °C) and above (55 °C) the LCST of PNIPAM are shown in table 1.

We attribute the changes in the diffusion coefficients at different temperatures to changes in the morphology of the PNIPAM chains at the QD surface. The hydrodynamic radii of the QDs depend on the conformation of the PNIPAM chains. Extended chains will increase the apparent hydrodynamic radius and, as a result, the diffusion coefficient will decrease. The most pronounced changes in the diffusion coefficients upon crossing the LCST were observed for samples R10 (more than ten fold) and R1 (more than five fold). For comparison, the diffusion coefficients were determined using DLS measurements as well (supporting information available at stacks.iop.org/Nano/22/265701/mmedia). The degrees of change in the diffusion coefficients are in good agreement as determined by both the FCS and DLS techniques. For the sample R25, however, light scattering experiments showed that the diffusion coefficient increased by a factor of ∼15 at T > LCST, while the FCS results suggested that the change was not remarkable. The long PNIPAM chains with low grafting density (0.4%) of the R25 sample probably resulted in an entangled morphology in the FCS probe volume, which was less sensitive to chain collapse at T > LCST, and therefore the diffusion coefficient was less affected.

In summary, the FCS measurements showed that crossing the LCST resulted in changes in both the optical and colloidal

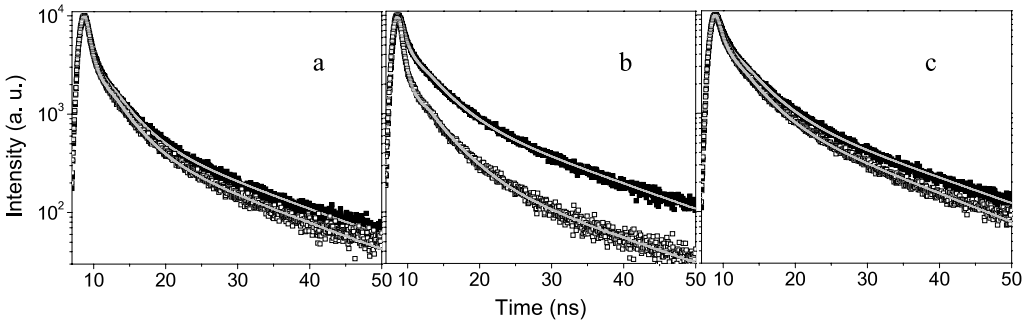

Figure 4. Luminescence decay curves of samples R1 (a), R10 (b) and R25 (c) measured at T < LCST (20 °C, ■) and T > LCST (55 °C, □) and fitted functions (gray curves).

Table 2. Components of the luminescence decays for QDs coated with R1, R10 and R25 and for unmodified QDs (in chloroform solution) measured at T < LCST (20 °C) and T > LCST (55 °C). Each measurement has 10% uncertainty. The fastest decay components, which were below the instrument response, are omitted in the table (<IR).

Sample	τ_1 (ps)	$\%\tau_1$	τ_2 (ns)	$\%\tau_2$	τ_3 (ns)	$\%\tau_3$	τ_{ave} (ns)
R1(20 °C)	100	42	3.2	30	15.5	28	5.3
R1(55 °C)	<IR*	51	3.2	28	15.1	21	4.1
R10(20 °C)	100	27	3.7	34	16.6	39	7.8
R10(55 °C)	<IR	91	3.9	6	17.1	3	0.8
R25(20 °C)	300	19	3.8	41	16.8	40	8.3
R25(55 °C)	200	24	3.5	40	14.9	36	6.8
QDs(20 °C)	460	13	4.3	31	22.2	56	13.8
QDs(55 °C)	340	17	4.6	30	22.6	53	13.4

properties of the QD/PNIPAM hybrid structures, as determined by the amplitudes and widths of the autocorrelation curves. The temperature-induced changes in the colloidal properties were confirmed also with the DLS measurements.

For further investigation of the influence of temperature on the optical properties of the samples, TCSPC measurements were performed at temperatures below and above the LCST. The luminescence decay curves were best fitted with a tri-exponential decay function [41]. Figure 4 displays the measured decays and the corresponding fits. The goodness of the fits (χ^2 value) varied from 1.2 to 2.0, which is very close to the ideal value of one.

The decay components (τ_1, τ_2, and τ_3) and their corresponding weights ($\%\tau_1$, $\%\tau_2$, and $\%\tau_3$, respectively) are shown in table 2. When compared to the unmodified QDs, the polymer coating process resulted in an overall decrease in the lifetimes. The most pronounced influence of polymer coating was observed as an increase of the relative weight of the fastest decay component τ_1 (table 2, column $\%\tau_1$), which is assigned to trapping processes caused by surface defects or impurities [42]. In contrast, the second and third time constants (τ_2 and τ_3, respectively) were nearly the same for all samples: 3.5 ± 0.5 ns and 16 ± 1 ns. It was previously reported that the second decay component τ_2 (3–4 ns) results from the presence of charged excitons and the third component τ_3 (∼15–23 ns) is taken to be the intrinsic lifetime, resulting from radiative electron–hole recombination [42]. Slight changes observed in τ_2 and τ_3 after polymer coating showed that the polymer did not interfere with the intrinsic photoluminescent properties of the QDs.

To facilitate the comparison between different samples, we define an average lifetime (τ_{ave}) as the intensity (I) average of the three decay components given by equation (4):

$$\tau_{ave} = \sum_{i=1}^{n} I_i \tau_i \Big/ \sum_{i=1}^{n} I_i \tag{4}$$

where τ_i is the decay time of the ith decay component with the intensity I_i. The QDs coated with the polymer having the longest PNIPAM chain (sample R25) exhibited the longest average lifetime of 8.3 ns, whereas those coated with the shortest PNIPAM chain had 5.3 ns average lifetime (see table 2).

Increasing the temperature above the LCST of PNIPAM resulted in a decrease in the average lifetime for all samples. The average lifetimes at T > LCST were dominated by the changes in the fastest decay component. The second and third decay components varied by ±0.5 ns at temperatures both below and above the LCST. The most pronounced effect of temperature on the average lifetime was observed for the sample R10, which has the highest PNIPAM content among all the samples.

It was previously shown that at temperatures above 200 K, a gradual decrease in the amplitude of the fast decay component of unmodified QDs is observed due to a nonradiative recombination process resulting from thermal activation [43]. However, the lifetime measurements we performed for the unmodified QDs did not show any remarkable change in the temperature range of 20–55 °C (table 2). In order to prove further that the observed change in lifetime as a function of temperature is mainly due to PNIPAM

chain collapse, we performed another control measurement using QDs modified with the same polymer coating, but the PNIPAM chains were replaced by a non-temperature-responsive polymer, poly(ethylene glycol) (PEG-QDs). The PEG-QDs showed no substantial change in their lifetimes as measured at 20 and 55 °C (see supporting information available at stacks.iop.org/Nano/22/265701/mmedia). These findings suggest that the observed changes in the average lifetimes of samples R1, R10 and R25 as a function of temperature are mainly due to PNIPAM chain collapse.

4. Conclusions

The colloidal and optical properties of QD/PNIPAM hybrid materials at temperatures below and above the LCST of PNIPAM were characterized. The FCS and TCSPC data provided new insights into the temperature-induced chain collapse of PNIPAM at $T >$ LCST. The QD/PNIPAM hybrids having different chain lengths of PNIPAM responded to changes in temperature to different extents depending on their PNIPAM content. Overall, the colloidal and optical stability of QD/PNIPAM hybrids was retained at $T >$ LCST. These findings suggest that surface engineering of QDs with thermo-responsive PNIPAM chains enables the realization of hybrid assemblies with thermo-switchable optical and colloidal properties as a function of PNIPAM chain length and grafting density. These materials are, in particular, attractive for biologically relevant sensing and separation applications, given that the LCST of PNIPAM is close to physiologically relevant temperatures.

Acknowledgment

This work was financially supported by the MESA+ Institute for Nanotechnology at the University of Twente.

References

[1] Henglein A 1989 *Chem. Rev.* **89** 1861
[2] Alivisatos A P 1996 *Science* **271** 933
[3] Bruchez M Jr, Moronne M, Gin P, Weiss S and Alivisatos A P 1998 *Science* **281** 2013
[4] Brus L 1991 *Appl. Phys.* A **53** 465
[5] Tomczak N, Janczewski D, Han M-Y and Vancso G J 2009 *Prog. Polym. Sci.* **34** 393
[6] Janczewski D, Tomczak N, Han M-Y and Vancso G J 2009 *Macromolecules* **42** 1801
[7] Ye J, Hou Y, Zhang G and Wu C 2008 *Langmuir* **24** 2727
[8] Zhou L, Gao C and Xu W 2009 *J. Mater. Chem.* **19** 5655
[9] Shiraishi Y, Adachi K, Tanaka S and Hirai T 2009 *J. Photochem. Photobiol.* A **205** 51
[10] Cheng Z, Liu S, Beines P W, Ding N, Jakubowicz P and Knoll W 2008 *Chem. Mater.* **20** 7215
[11] Gil E S and Hudson S M 2004 *Prog. Polym. Sci.* **29** 1173
[12] Schild H G 1992 *Prog. Polym. Sci.* **17** 163
[13] Fujishige S, Kubota K and Ando I 1989 *J. Phys. Chem.* **93** 3311
[14] Wei H, Cheng S-X, Zhang X-Z and Zhuo Z-X 2009 *Prog. Polym. Sci.* **34** 893
[15] Mizutani A, Kikuchi A, Yamato M, Kanazawa H and Okano T 2008 *Biomaterials* **29** 2073
[16] Ozturk N, Girotti A, Kose G T, Rodriguez-Cabello J C and Hasirci V 2009 *Biomaterials* **30** 5417
[17] Doose S, Tsay J M, Pinaud F and Weiss S 2005 *Anal. Chem.* **77** 2235
[18] Murcia M J, Shaw D L, Long E C and Naumann C A 2008 *Opt. Commun.* **281** 1771
[19] Zhang P, Li L, Dong C, Qian H and Ren J 2005 *Anal. Chim. Acta* **546** 46
[20] Tagit O, Janczewski D, Tomczak N, Han M-Y, Herek J L and Vancso G J 2010 *Eur. Polym. J.* **46** 1389
[21] Bacia K, Scherfeld D, Kahya N and Schwille P 2004 *Biophys. J.* **87** 1034
[22] Kinjo M 1998 *Anal. Chim. Acta* **365** 43
[23] Schwille P 2001 *Cell Biochem. Biophys.* **34** 383
[24] Sengupta P, Garai K, Balaji J, Periasamy N and Maiti S 2003 *Biophys. J.* **84** 1977
[25] Hess S T, Huang S, Heikal A A and Webb W W 2002 *Biochemistry* **41** 697
[26] Heuff R F, Cramb D T and Marrocco M 2008 *Chem. Phys. Lett.* **454** 257
[27] Heuff R F, Swift J L and Cramb D T 2007 *Phys. Chem. Chem. Phys.* **9** 1870
[28] Akcakir O, Therinnen J, Belomoin G, Barry N, Muller J D, Gratton E and Nayfeh M 2000 *Appl. Phys. Lett.* **76** 1857
[29] Pellegrino T, Manna L, Kudera S, Liedl T, Koktysh D, Rogach A L, Keller S, Rädler J, Natile G and Parak W J 2004 *Nano Lett.* **4** 703
[30] Adelsberger J *et al* 2010 *Macromolecules* **43** 2490
[31] Lakowicz J R 2006 *Principles of Fluorescence Spectroscopy* (New York: Springer)
[32] Pelton M, Smith G, Scherer N F and Marcus R A 2007 *Proc. Natl Acad. Sci.* **104** 14249
[33] Xie X S and Trautman J K 1998 *Annu. Rev. Phys. Chem.* **49** 441
[34] Weiss S 1999 *Science* **283** 1676
[35] Yamada T, Goushi K, Xu X and Otomo A 2008 *Thin Solid Films* **517** 1507
[36] Magde D, Elson E and Webb W W 1972 *Phys. Rev. Lett.* **29** 705
[37] Wang M, Felorzabihi N, Guerin G, Haley J C, Scholes G D and Winnik M A 2007 *Macromolecules* **40** 6377
[38] Dong C, Huang X and Ren J 2008 *Ann. New York Acad. Sci.* **1130** 253
[39] Ito S, Toitani N, Pan L, Tamai N and Miyasaka H 2007 *J. Phys.: Condens. Matter* **19** 486208
[40] Larson D R, Zipfel W R, Williams R M, Clark S W, Bruchez M P, Wise F W and Webb W W 2003 *Science* **300** 1434
[41] Sadhu S and Patra A 2008 *Chem. Phys. Chem.* **9** 2052
[42] Salman A A, Tortschanoff A, van der Zwan G, van Mourik F and Chergui M 2009 *Chem. Phys.* **357** 96
[43] Lee W Z, Shu G W, Wang J S, Shen J L, Lin C A, Chang W H, Ruaan R C, Chou W C, Lu C H and Lee Y C 2005 *Nanotechnology* **16** 1517